

Electronic Supplementary Information

**Natural Abundance  $^{13}\text{C}$  and  $^{15}\text{N}$  Solid-State NMR Analysis of Paramagnetic  
Transition-Metal Cyanide Systems**

Pedro M. Aguiar<sup>†</sup>, Michael Katz<sup>‡</sup>, Daniel B. Leznoff<sup>‡</sup>, Scott Kroeker<sup>†\*</sup>

<sup>†</sup> Department of Chemistry, University of Manitoba, Winnipeg, Manitoba, Canada

<sup>‡</sup> Department of Chemistry, Simon Fraser University, Vancouver, British Columbia, Canada

**Table S1** Selected Bond Lengths (Å) and Angles(°) for **8**.<sup>a</sup>

Zn(1) – N(1*)	2.362(17)	Zn(1) – N(3*)	2.135(9)
Zn(1) – N(3'')	2.135(9)	Zn(1) – N(3')	2.135(9)
Zn(1) – N(1)	2.362(17)	Zn(1) – N(3)	2.135(9)
Au(1) – Au(2\$)	3.2201(6)	Au(1) – Au(2)	3.2201(6)
N(1*) – Zn(1) – N(3*)	89.5(4)	N(1*) – Zn(1) – N(3'')	89.5(4)
N(3*) – Zn(1) – N(3'')	97.7(5)	N(1*) – Zn(1) – N(3')	90.5(4)
N(3*) – Zn(1) – N(3')	82.3(5)	N(3'') – Zn(1) – N(3')	180
N(1*) – Zn(1) – N(1)	180	N(3*) – Zn(1) – N(1)	90.5(4)
N(3'') – Zn(1) – N(1)	90.5(4)	N(3') – Zn(1) – N(1)	89.5(4)
N(1*) – Zn(1) – N(3)	90.5(4)	N(3*) – Zn(1) – N(3)	179.995
N(3'') – Zn(1) – N(3)	82.3(5)	N(3') – Zn(1) – N(3)	97.7(5)
N(1) – Zn(1) – N(3)	89.5(4)	Zn(1) – N(1) – C(1)	150.4(14)
Zn(1) – N(3) – C(3)	106.4(8)		

<sup>a</sup>Symmetry transformations : \*: 1-x, -y, 3-z; '': 1-x, y, 3-z; ': x, -y, z; \$: x, y, 1+z

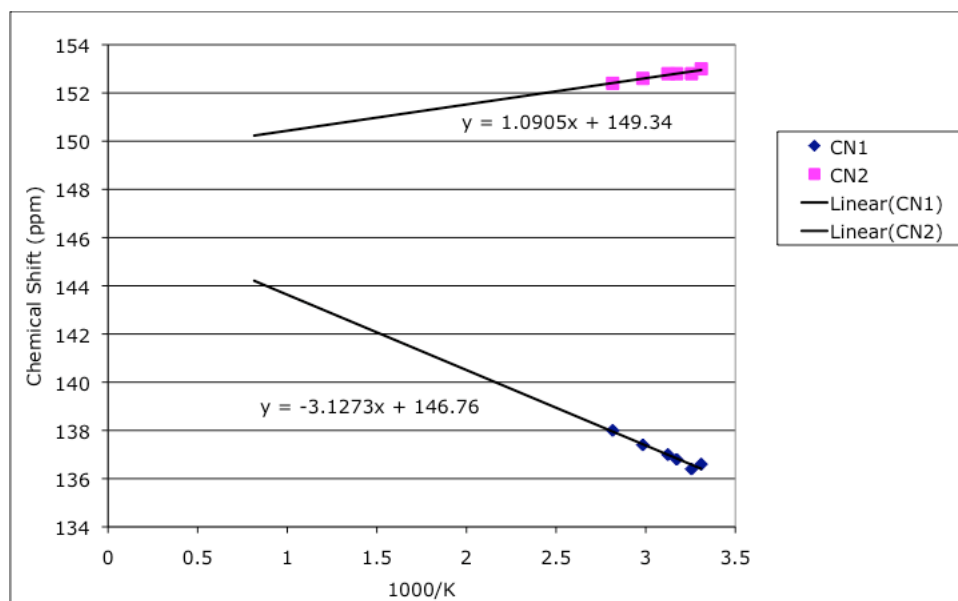


**Figure S1:** The temperature dependence of the two  $^{13}\text{C}$  cyanide signals for compound 1.

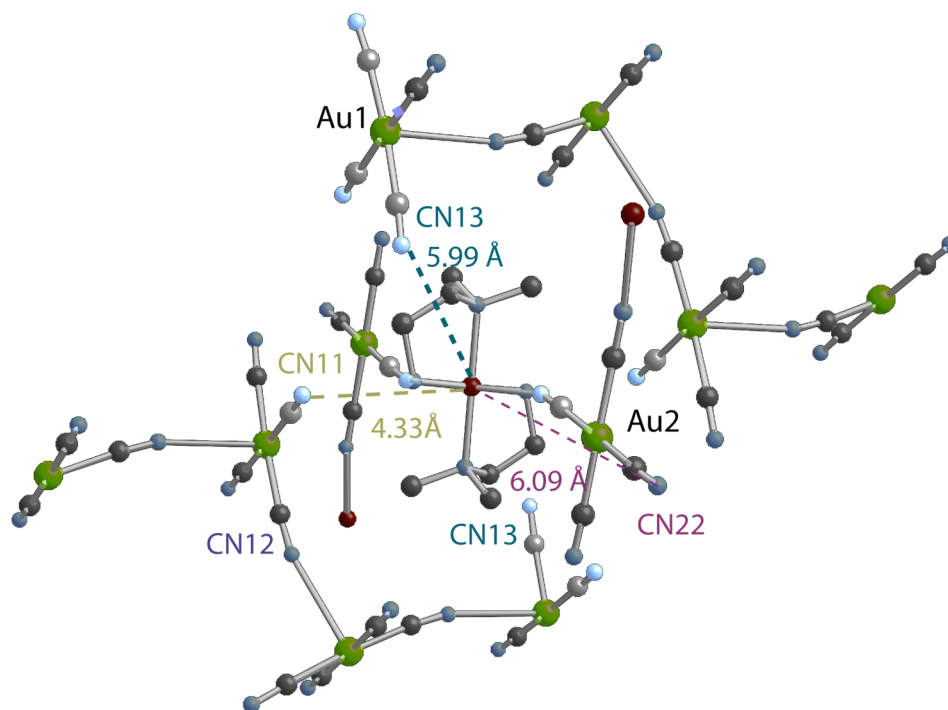


**Figure S2:** Structure of compound 3 along with selected nitrogen to copper distances.

**Table S2: Results of  $^{13}\text{C}$  variable-temperature experiments.**

Sample				
Site	$\delta_{\text{diam}}$ (ppm)	Slope (ppm/1000 K)	$^{13}\text{C}$ $\rho_{\alpha\beta}$ (a.u.)	$R^2$
[Cu(en) <sub>2</sub> ][Hg(CN) <sub>2</sub> Cl] <sub>2</sub>				
CN1	147 ± 2	-3.1273	-0.000089	0.958
CN2	149 ± 2	1.0905	0.000031	0.935
en (-CH <sub>2</sub> -)	n.d.			
[Cu(en) <sub>2</sub> ][Ag <sub>2</sub> (CN) <sub>3</sub> ][Ag(CN) <sub>2</sub> ]				
CN21	153 ± 2	-2.28749	-0.000065	0.937
CN21 <sup>a</sup>	153 ± 2	-2.28749	-0.000065	0.937
CN11		0		
CN11 <sup>a</sup>		0		
CN20		0		
en (-CH <sub>2</sub> -)	43 ± 13	-108.68957	-0.003083	0.993
[Cu(en) <sub>2</sub> ][Au(CN) <sub>2</sub> ] <sub>2</sub>				
CN1	152 ± 2	-8.1537	-0.000231	0.963
CN2	152 ± 2	5.7818	0.000164	0.954
en (-CH <sub>2</sub> -)	-40 ± 30	-81.009	-0.002298	0.891

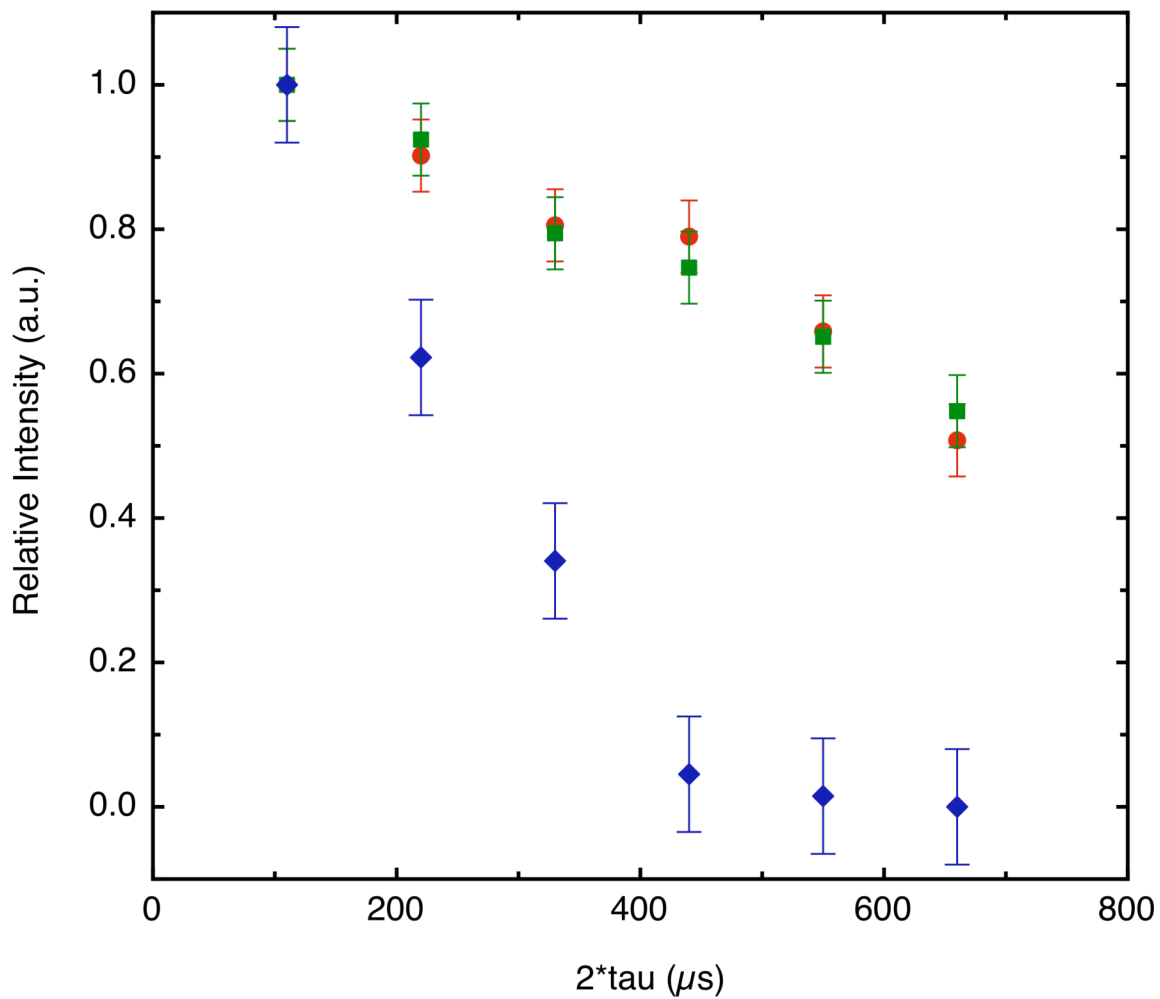


Figure S3: Spin-spin relaxation data for sample  $[\text{Cu}(\text{en})_2[\text{Zn}(\text{NC})_4(\text{CuCN})_2]$ . The intensities for the signals at 182 (red circles) and 165 ppm (green squares) signals decay much more slowly than the 122 ppm signal (blue diamonds).

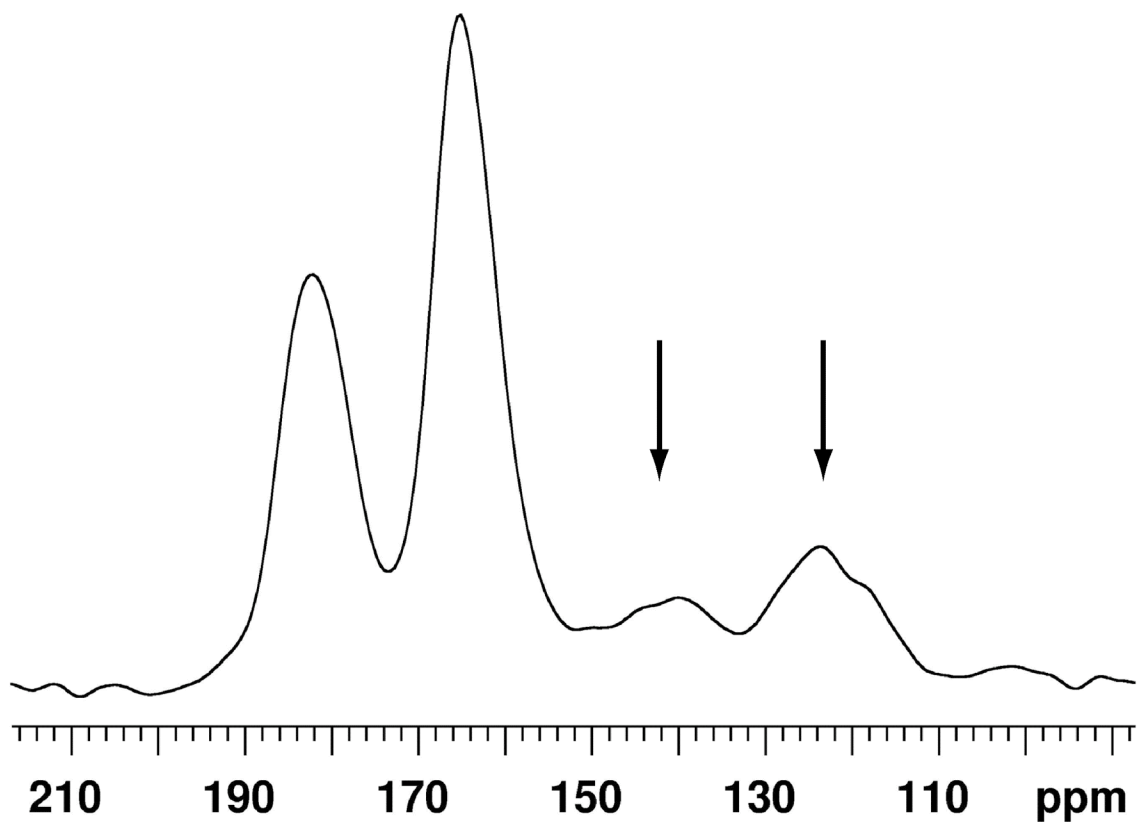


Figure S4:  $^{13}\text{C}$  MAS of  $[\text{Cu}(\text{en})_2[\text{Zn}(\text{NC})_4(\text{CuCN})_2]$  showing the splitting of the low-frequency peak upon changing the temperature.

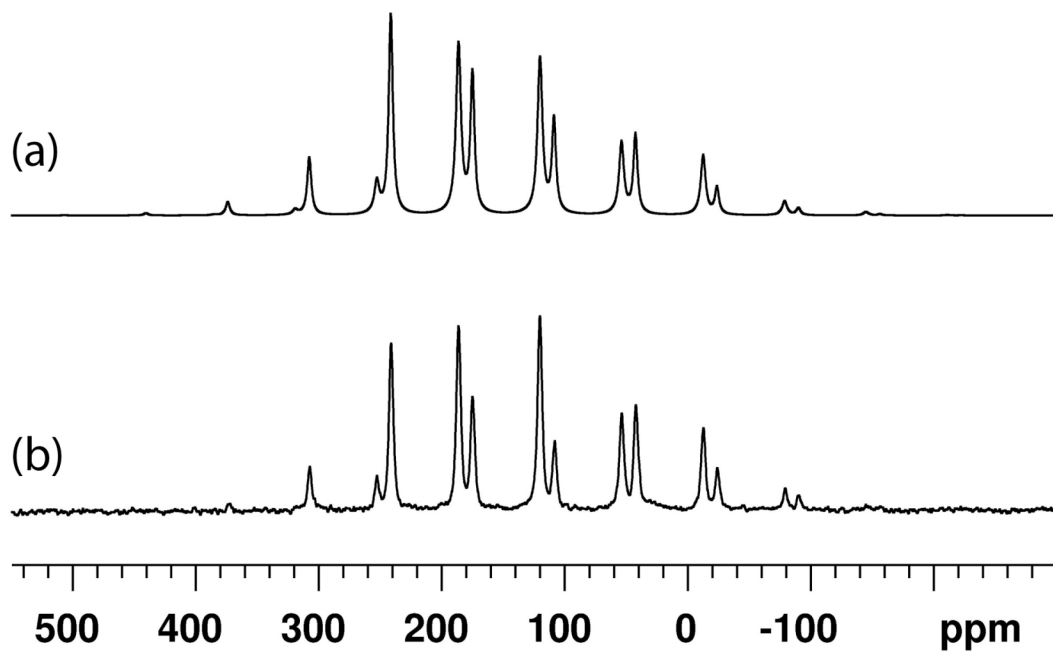


Figure S5: Simulated (a) and experimental (b) spectra for compound 7 acquired at 10 kHz spinning.

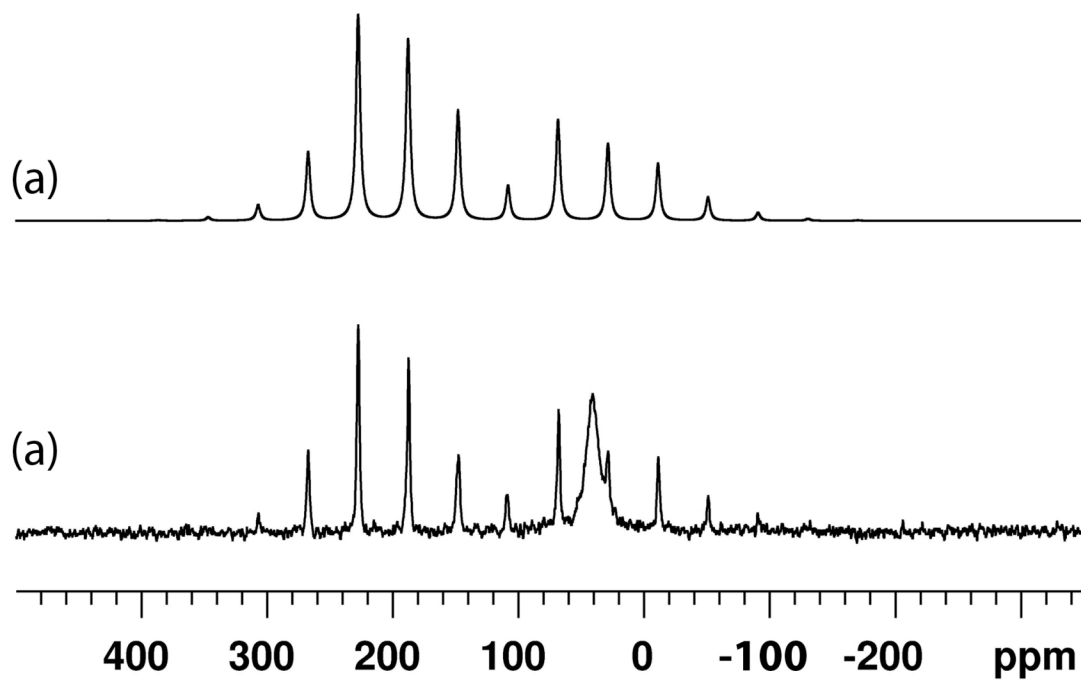


Figure S6: Simulation (a) and experimental (b) spectra for compound 8 acquired at 6 kHz spinning.